Wideband Microwave Filters Using Ferromagnetic Resonance Tuning in Flip-Chip YIG-GaAs Layer Structures

Chen S. Tsai[1,2], *Life Fellow, IEEE*, and Gang Qiu[1]

[1]Department of Electrical Engineering and Computer Science, and Institute of Surface and Interface Sciences, University of California, Irvine, CA 92697 USA

[2]Institute of Electrooptics Engineering, National Taiwan University, Taipei, Taiwan

In this paper the most recent advances on ferromagnetic resonance (FMR)-based wideband microwave band-stop and band-pass filters using flip-chip yttrium iron garnet (YIG)/gadolinium gallium garnet (GGG)- gallium arsenide (GaAs) layer structures are reported. Specifically, simultaneous enhancement in tunable bandwidths and peak absorption levels by utilizing the meander microstrip line with step-impedance low-pass filter design together with inhomogeneous magnetic field has been accomplished. For example, an ferromagnetic resonance absorption frequency tuning range of 5 to 21 GHz, an absorption level of −35.5 dB and a corresponding 3 dB absorption bandwidth as large as 1.70 GHz, centered at 20.3 GHz, have been accomplished with the band-stop filter. For the band-pass filter large tuning ranges for the center frequency (5.90–17.80 GHz), the pass-band bandwidth (1.27–2.08 GHz) as well as the two guarding stop-bandwidths (0.45–1.70 GHz), and an out-of-band rejection of −33.5 dB were demonstrated. A good agreement between the simulation and experimental results has been achieved. Finally, some desirable measurement data on the microwave power capability and the magnetic tuning speed of the filters has also been obtained.

***Index Terms*—Bandpass filters, bandstop filters, ferromagnetic resonance, tunable YIG filters.**

I. Introduction

TUNABLE FILTERS are among the essential devices used in detecting and controlling the spectrums of RF (radio frequency) signals in radar and communication systems [1]–[3]. For example, tunable wideband microwave band-stop filters that possess frequency selectivity with high absorption level and large absorption bandwidth are required for suppression of frequency parasitics, spurious bands or harmonics. Also, tunable wideband microwave band-pass filters perform critical function in the scanner receiver of electronic support measures (ESM) systems which detects and classifies incoming signals for electronic countermeasures (ECM) systems that in turn provide appropriate countermeasures such as jamming. In recent years, there have been active efforts toward the realization of ferromagnetic thin-film-based tunable microwave filters and devices in high frequency applications [4]–[12]. Ferromagnetic thin-film-based planar microwave filters possess the desirable capability of high-speed electronic tunability, using magnetic field, for very high carrier frequency and very large bandwidth.

In this paper, the most recent advances on wideband microwave band-stop and band-pass filters that utilized microstrip meander-lines with multi-element step-impedance low-pass filter (SILPF), in lieu of 50 Ω microstrips, together with non-uniform bias magnetic fields [10] for simultaneous enhancement of the ferromagnetic resonance absorption level and the absorption bandwidth in flip-chip yttrium iron garnet/gadolinium gallium garnet-gallium arsenide (YIG/GGG-GaAs) layer structures are reported. Fig. 1 shows the basic device configuration of a flip-chip YIG/GGG-GaAs-based tunable microwave band-stop filter [6], [10]. A YIG/GGG layer is laid upon the GaAs-based microstrip line. An incoming microwave is coupled into the YIG/GGG layer and the maximum coupling and, thus, peak absorption of the microwave power occurs when its carrier frequency coincides with the ferromagnetic resonance (FMR) frequency of the YIG/GGG layer. The external bias magnetic field (H_0) dependence of the ferromagnetic resonance frequency (f_r) is given by [4]

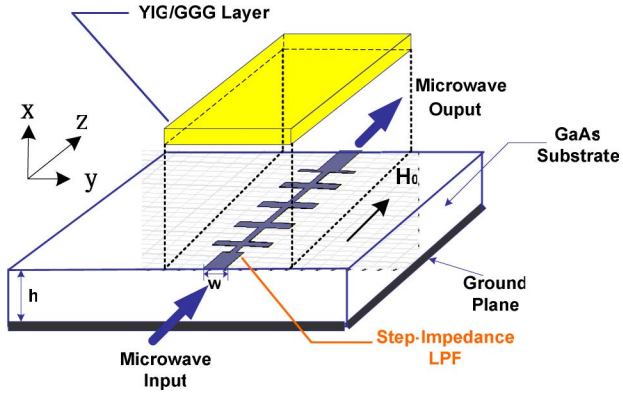

Fig. 1. Tunable microwave band-stop filter using YIG-GaAs layer flip-chip configuration.

$$f_r(H_0) = \gamma\sqrt{(H_{\rm an} + H_0)(H_{\rm an} + H_0 + 4\pi M_s)} \qquad (1)$$

where γ is the gyromagnetic ratio, and $4\pi M_s$ and H_{an} are, respectively, the saturation magnetization and the anisotropy field of the YIG film.

Both the resulting band-stop filters and the band-pass filters using a pair of such band-stop filters in cascade with large tuning ranges for the operation center frequencies and the bandwidths in the stop- and pass-bands and large power absorption levels were constructed and studied.

Manuscript received October 27, 2008. Current version published February 11, 2009. Corresponding author: C. S. Tsai (e-mail: cstsai@uci.edu).

Color versions of one or more of the figures in this paper are available online at http://ieeexplore.ieee.org.

Digital Object Identifier 10.1109/TMAG.2008.2010466

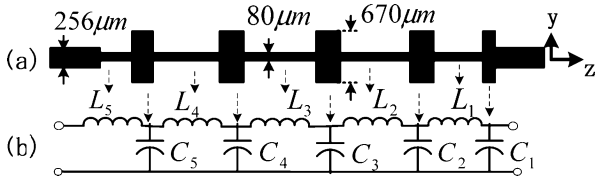

Fig. 2. A 10-element step impedance low-pass filter.

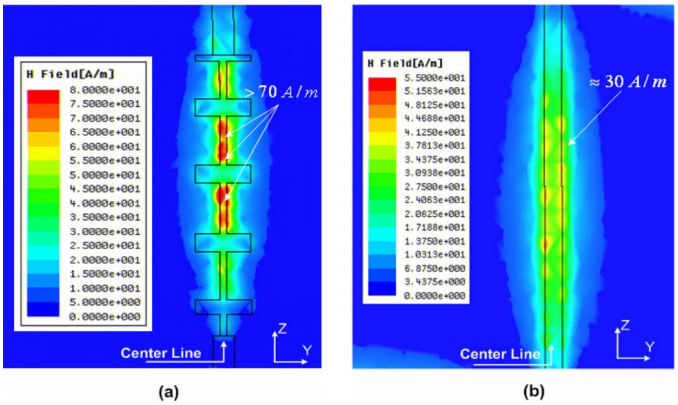

Fig. 3. Simulated H-field distributions at $f = 8.5$ G along (a) the 10-segment SILPF, and (b) the 50 Ω microstrip.

II. Tunable Wideband Microwave Band-Stop Filters

A. Enhancement for Microwave Coupling Using SILPF Design

The 10-element SILPF designed for this purpose has 256 um wide line as a 50 Ω transmission line and the 670 um and 80 um wide lines as the low and high characteristic impedance lines of 30 Ω and 75 Ω, respectively, corresponding to the shunt capacitors and the series inductors (see Fig. 2(a) and (b)) [10].

The S-parameters simulations using *Ansoft HFSS* show that such 10-element SILPF is an efficient transmission line over a frequency band of 0 to 26.5 GHz. *Ansoft HFSS* was then used to simulate the ac magnetic fields (H-fields) on the surface of the GaAs substrate at 8.5 GHz along the 10-element SILPF and the 50 Ω microstrip, respectively, in Fig. 3(a) and (b). Fig. 3(a) clearly shows that the H-fields of the propagating microwaves are heavily concentrated in each inductive element (note that the narrow microstrip segments are the high characteristic impedance lines corresponding to the series inductors). Specifically, the H-field intensity in the inductive line segments is seen to be greater than 70 A/m in contrast to a much lower H-field intensity of 30 A/m along the 50 Ω microstrip. Such stronger local H-fields result in enhanced coupling between the magnetic fields of the microwaves and the precessing magnetic dipoles in the YIG/GGG over-layer, and thus the level of microwave absorption.

In the experiments, a YIG/GGG layer (with 6.8 μm thick YIG) sample of dimensions 6.5×8.0 mm^2 in the Y and Z directions (see Fig. 1) was laid upon the two types of GaAs-based microstrip transmission lines presented above to realize the band-stop filter configuration of Fig. 1. The 50 Ω microstrip and the 10-element SILPF, each with design length of 5.7 mm, were fabricated separately on the 350 μm thick GaAs substrates

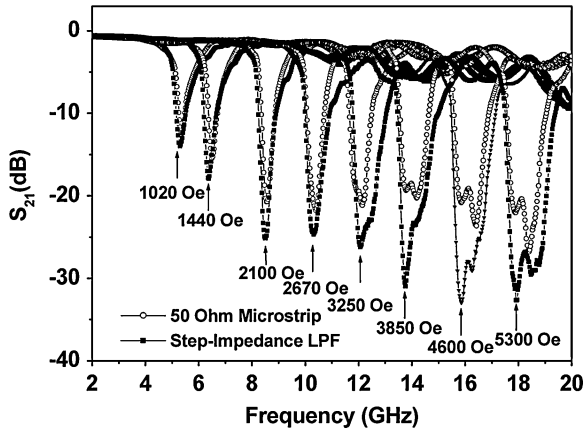

Fig. 4. Measured transmission loss (S_{21}) of the YIG/GGG-GaAs-based microwave band-stop filter using the 50 Ω microstrip and the 10-element SILPF.

in order to compare their microwave power absorptions at the ferromagnetic resonance frequencies. The flip-chip YIG/GGG-GaAs layer structure was then inserted in a uniform bias magnetic field (H_0) with its direction parallel to that of the microwave propagation as depicted in Fig. 1. The S-parameters for the completed device were measured using HP 8510 C Network Analyzer.

The microwave transmission characteristics of the band-stop filter in the frequency range of 2.0–20.0 GHz using the two types of transmission lines were measured and compared in Fig. 4. Clearly, enhanced peak ferromagnetic resonance absorptions in the flip-chip YIG/GGG-GaAs layer structure were accomplished in a base band as large as 5.0 to 20.0 GHz using the 10-element SILPF.

B. Electronic Tunability of the Band-Stop Filters

Fig. 5 shows the components of the magnetic circuit that were used to facilitate electronic tuning of the band-stop filter. Each of the disk-shape NdFeB permanent magnet has the dimensions of $0.5''$ in thickness and $0.75''$ in diameter. The electric wire used for the solenoids is of the size of 28 a.w.g. and the number of turns in each coil is 820. The pair of solenoids was wrapped around the NdFeB permanent magnets to facilitate electronic tuning of the magnetic field in the air gap. The measured changes of magnetic fields (ΔH) in the air gap versus the DC currents in the coils, with the air gap distance as a parameter, are shown in Fig. 6. Table I lists the measured magnetic fields and maximum ΔH in the center of air gap at four discrete air gaps of 11, 17.1, 24.1, and 30.6 mm, and its corresponding maximum tuning ranges of the ferromagnetic resonance frequencies. Using different combinations of the air gap and the current in the coils, a tuning range as large as 5.5–18.8 GHz for the ferromagnetic resonance absorption frequencies was realized.

It is of interest to determine the time it would take to tune electronically the dc magnetic field, and thus the tuning speed of the ferromagnetic resonance absorption frequency. The electrical parameters of the coils were measured by using Agilent 4294A impedance analyzer. The measured values of the inductance, capacitance, and resistance are 12.2 mH, 165.5 pF, and 20 Ω, respectively. A step-function voltage (0–2 Vpp) from a function generator was used to drive the coil. A response time (rise

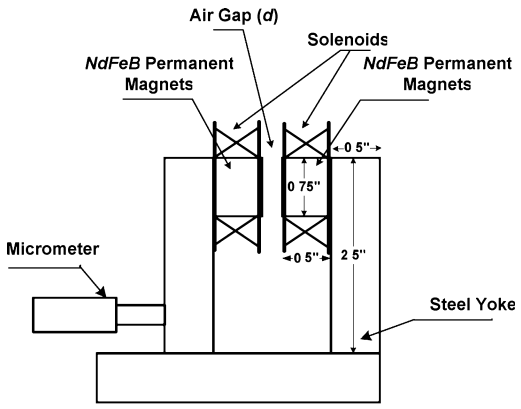

Fig. 5. The sketch of the electromagnet.

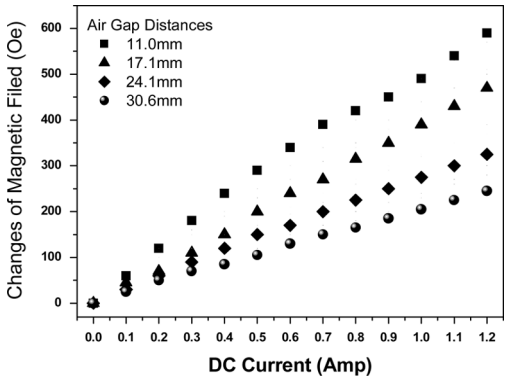

Fig. 6. The measured changes of magnetic fields (ΔH) in the air gap versus the DC current in the coils with the air gap distance as a parameter.

or fall time) of 43 μs was measured in a series resistor-inductor (coil) circuit with the series resistance of 270 Ω. The measured response time was found to be in good agreement with the calculated values based on the measured inductance, capacitance, and resistance of the coil.

C. Power Handling Capability of the Band-Stop Filters

The power handling capability of the fabricated band-stop filter was also measured. The microwave transmission characteristics of the band-stop filter using one segment microstrip SILPF were measured at different microwave power input levels in the range of 1–500 mW. The measurement data (see Fig. 7) shows no obvious changes at the four discrete microwave power input levels (1 mW, 10 mW, 100 mW, and 500 mW) in the important quantities of ferromagnetic resonance frequencies, power absorption levels, and ferromagnetic resonance absorption spectrums.

D. Measured Transmission Characteristics of the Band-Stop Filters

Microwave band-stop filters with desirable performances, i.e., wideband frequency selectivity with high peak absorption level and large absorption bandwidth, were realized using a four-segment microstrip meander-line constructed by the same 10-element SILPFs together with a 2-D non-uniform bias magnetic field [10]. The arrangement for facilitating 2-D

TABLE I
MEASURED MAGNETIC FIELDS AND MAXIMUM ΔH IN THE CENTER OF THE AIR GAP AND THE MAXIMUM TUNING RANGES OF THE BAND-STOP FILTERS

Air Gap(mm)	11.0	17.1	24.1	30.6
Center Magnetic Field (Oe)	5,200	3,250	2,000	1,425
ΔH_{max}@DC Current $= \pm 1.2$ A	$\pm$590	$\pm$470	$\pm$325	$\pm$245
Maximum Tuning Range (GHz)	15.4-18.8	10.2-12.9	7.0-9.0	5.5-7.0

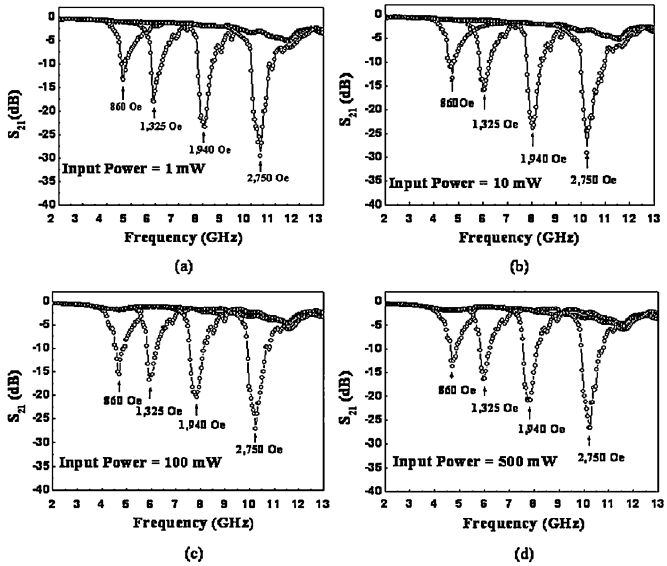

Fig. 7. (a) Measured transmission characteristics of the band-stop filter at different microwave power levels of (a) 1 mW (b) 10 mW (c) 100 mW, and (d) 500 mW.

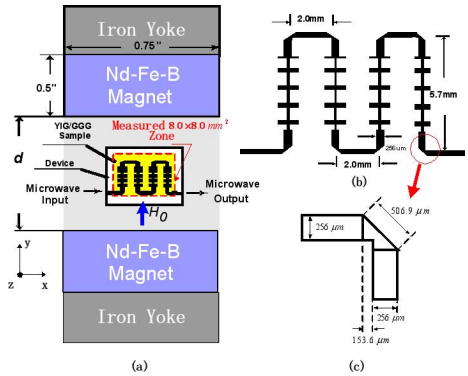

Fig. 8. (a) The arrangement for facilitating non-uniform bias magnetic fields in YIG/GGG layer, (b) the layout of the four-segment microstrip meander-line, and (c) layout of the mitered 90° bend segment.

non-uniform bias magnetic fields in YIG/GGG layer, the layout of the four-segment microstrip meander line and the optimized mitered 90° bend segment are shown in Fig. 8(a) (b) and (c), respectively. Such band-stop filter, using 6.8 μ thick YIG sample, has demonstrated a large tuning range in peak absorption frequency of 5.0 to 21.0 GHz and an absorption level of -35.5 dB together with a corresponding 3 dB bandwidth as large as 1.70 GHz (see Fig. 9).

Most recently, an even higher peak absorption level and much larger absorption bandwidth of the band-stop filter were realized using a 100 μ thick YIG sample (6.5 $\times$ 8.0 mm in the Y and Z

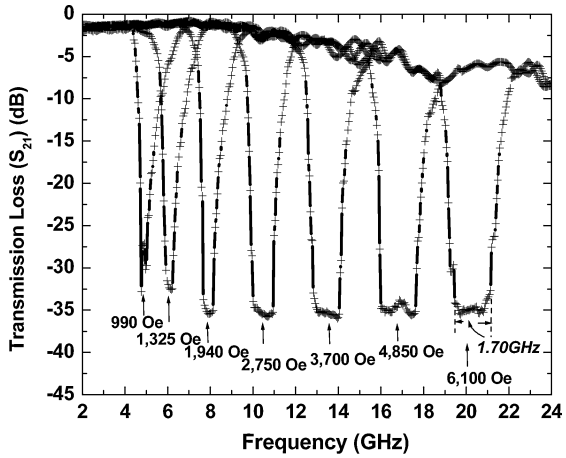

Fig. 9. Measured S_{21} of the band-stop filter using the microstrip meander line with four segments of SILPF together a 6.8 μm YIG sample.

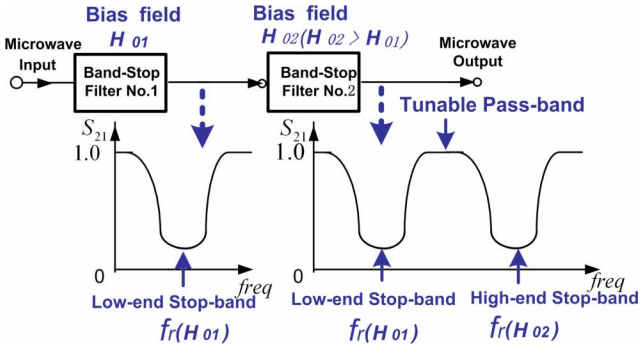

Fig. 10. Realization of the tunable band-pass filter using a pair of band-stop filters in cascade.

directions). The results will be reported separately in the near future.

III. Tunable Wideband Microwave Band-Pass Filters

A. Device Architecture and Simulation

Microwave band-pass filters with large tuning ranges for both the center frequency and the pass-band bandwidth were realized by using a pair of aforementioned band-stop filters in cascade (see Fig. 10) in which different non-uniform bias magnetic fields $(H_{02} > H_{01})$ were applied [12]. *Ansoft HFSS* was used in the design and simulation of the band-pass filter that incorporates four-segment microstrip meander-lines and 2-D non-uniform bias magnetic fields [12]. A good agreement between the experiment results and the simulation results in the center frequency and the bandwidths of the pass-band and the two guarding stop-bands has been achieved [11], [12].

B. Measured Transmission Characteristics of the Band-Pass Filters

Large tuning ranges in the pass-band center frequency (5.90–17.80 GHz) and the bandwidth (1.27–2.08 GHz) of the band-pass filter, using 6.8 μm thick YIG sample, were measured most recently (see Fig. 11). Note that the measured transmission characteristics lower than the low-end stop-band and higher

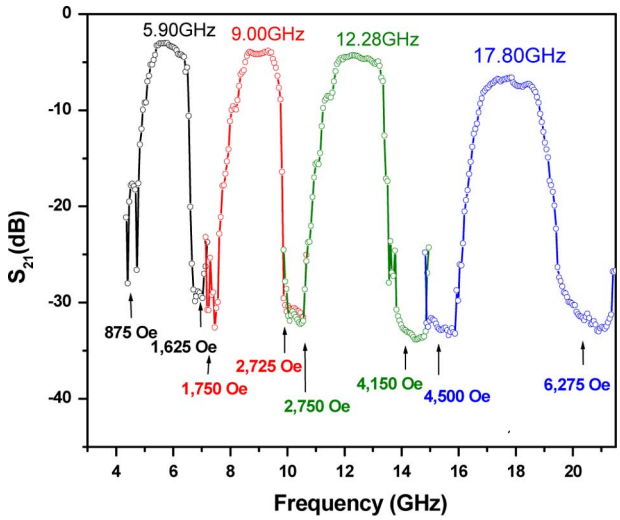

Fig. 11. Measured transmission characteristics of the tunable band-pass filter in the range of 5.90–17.8 GHz.

TABLE II
Measured Insertion Losses and Band-Widths of The Band-Pass Filter of Fig. 10

Pass-Band Center Frequency (GHz)	5.90	9.00	12.28	17.80
BW@-3dB (MHz)	1,270	1,300	1,730	2,080
Insertion Loss (dB)	- 3.1	- 3.9	-4.2	-6.6

than the high-end stop-band are not plotted in the figure, i.e., only the two stop-bands and the pass-band are plotted. The measured pass-band bandwidths and insertion losses are listed in Table II. Note that the insertion loss can be reduced by utilization of a meander microstrip line with improved design. Finally, as with the band-pass filters presented in Section II-C, the transmission characteristics of the band-pass filters at the two guarding stop-bands were measured at the microwave power of 1, 10, 100, and 500 mW. No significant changes in the ferromagnetic resonance frequency and the corresponding peak power absorption level and absorption spectrum were observed even at the highest power level of 500 mW.

IV. Conclusion

The microwave band-stop filters using the flip-chip YIG-GaAs layer structure and a microstrip meander-line with multiple segments of the SILPFs in a non-uniform bias magnetic field have provided simultaneously enhanced ferromagnetic resonance peak power absorption level and large absorption bandwidth. The microwave band-pass filters with wide tuning ranges in operation center frequency and pass-band bandwidths as well as large absorption bandwidth and power absorption level in the two guarding stop-bands have also been realized using a pair of the band-stop filters in cascade. Both types of filters have demonstrated desirable capabilities in microwave power level and tuning speed. Such magnetically tunable filters, when fully developed, should find applications in wideband microwave communication and signal processing systems.

ACKNOWLEDGMENT

This work was supported by UC Discovery Program and Wang, NMR Inc. The YIG/GGG samples used were furnished by Shin-Etsu Chemical Co., Japan.

REFERENCES

[1] G. L. Matthaei, "Magnetically tunable band-stop filters," *IEEE Trans Microw. Theory Tech.*, vol. MTT-13, no. 2, pp. 203–212, Mar. 1965.

[2] I. C. Hunter, L. Billonet, B. Jarry, and P. Guillon, "Microwave filters—applications and technology," *IEEE Trans Microw. Theory Tech.*, vol. 50, no. 3, pp. 794–805, Mar. 2002.

[3] J. D. Adam, L. E. Davis, G. F. Dionne, E. F. Schloemann, and S. N. Stitzer, "Ferrite devices and materials," *IEEE Trans Microw. Theory Tech.*, vol. 50, no. 3, pp. 721–737, Mar. 2002.

[4] C. S. Tsai and J. Su, "A wideband electronically tunable magnetostatic wave notch filter in yttrium iron garnetgallium arsenide material structure," *Appl. Phys. Lett.*, vol. 74, pp. 2079–2080, 1999.

[5] B. K. Kuanr, D. L. Marvin, T. M. Christensen, R. E. Camley, and Z. Celinski, "High-frequency magnetic microstrip local bandpass filters," *Appl. Phys. Lett.*, vol. 87, 2005.

[6] C. S. Tsai, G. Qiu, H. Gao, L. W. Yang, G. P. Li, S. A. Nikitov, and Y. Gulyaev, "Tunable wideband microwave band-stop and band-pass filters using YIG/GGG-GaAs layer structures," *IEEE Trans. Magn.*, vol. 41, no. 10, pp. 3568–3570, Oct. 2005.

[7] V. G. Harris, Z. Chen, Y. Chen, S. Yoon, T. Sakai, A. Gieler, A. Yang, Y. He, K. S. Ziemer, N. X. Sun, and C. Vittoria, "Ba-hexaferrite films for next generation microwave devices," *J. Appl. Phys.*, vol. 99, 2006.

[8] C. E. Patton, M. Z. Wu, K. R. Smith, and V. I. Vasyuchka, "Nonlinear ferrite film microwave processing for advanced communications—Physics and devices," *Ferroelectrics*, vol. 342, pp. 101–106, 2006.

[9] J. Das, B. A. Kalinikos, A. R. Barman, and C. E. Patton, "Multifunctional dual-tunable low loss ferrite-ferroelctric heterostructures for microwave devices," *Appl. Phys. Lett.*, vol. 91, pp. 172516-1–172516-3, 2007.

[10] G. Qiu, M. Kobayashi, B. T. Wang, and C. S. Tsai, "Enhanced microwave ferromagnetic resonance absorption and bandwidth using a microstrip meander line with step-impedance low pass filter in a yttrium iron garnet—Gallium arsenide layer structure," in *52nd Annu. Conf. MMM*, Tampa, FL, Nov. 5–9, 2007, Paper EH-03, Also, *J. Appl. Phys.*, vol. 103 07E915, Apr. 1, 2008.

[11] A. Cismaru and R. Marcelli, "CPW cascaded magnetostatic-wave bandstop resonators," *IEEE Trans. Magn.*, vol. 42, pp. 3347–3349, 2006.

[12] G. Qiu, C. S. Tsai, B. T. Wang, and Y. Zhu, "A YIG/GGG/GaAs-based magnetically tunable wideband microwave band-pass filter using cascaded band-stop filters," presented at the International Magnetics Conf., Madrid, Spain, May 5–8, 2008.